Mühendis ve Makina / Engineer and Machinery
https://dergipark.org.tr/tr/pub/muhendismakina

COMPARISON OF MACHINABILITY OF AL-4.5%CU/TIB2/3P MMC FOR MULTI-LAYER COATED INSERT: VALIDATED FEM AND STATISTICAL APPROACHES

Erkan ÖZTÜRK[1*]

[1] Department of Mechanical Engineering, Faculty of Engineering, Ondokuz Mayıs University, Samsun

ORCID No : http://orcid.org/0000-0002-7056-718X

Keywords

Multi-layer coated tool, finite element method, grey relation analysis

Abstract

Aluminum-based Metal Matrix Composites (MMC) are commonly used in metal-cutting applications due to their better mechanical and physical properties, such as high strength, hardness, and low weight. Also, modern coating applications, especially multi-layer coated tools, have cutting-edge potential for relieving the difficulties of machining MMCs to improve insert performances. Therefore, this study aimed to reveal the turning Al-4.5%Cu/TiB2/3p performance of the multi-layer coated cemented carbide insert with verified FEM and statistical approaches. Different coating materials, two and three of which were soft and hard, were appointed at different thicknesses and sequences in the design of experimentally calibrated simulations. The Grey Relation Analysis (GRA) was set to investigate the multi-layer coated insert performance for turning the MMC concerning the resultant cutting forces (FR) and maximum insert temperature (Tmax). The optimal multi-layered coating was found at levels 4-2-4-3-2 for the factors of coating materials: tungsten disulfide (WS2), molybdenum disulfide (MoS2), titanium nitride (TiN), aluminum oxide (Al2O3), and titanium carbo-nitride (TiCN), respectively. The contribution rates of each factor were significant concerning the General Linear Model (GLM) at 47.13% and 24.43% for WS2 and Al2O3 coatings materials, respectively. In the future, multi-layered coatings can be a valuable solution for the difficulties of machining the MMCs.

* erkan.ozturk@omu.edu.tr
doi : 10.46399/muhendismakina.1329342

AL-4.5%CU/TIB2/3P MMK'NIN ÇOK KATMANLI KAPLAMALI KESİCİ TAKIMLARLA İŞLENEBİLİRLİĞİNİN KARŞILAŞTIRILMASI: DOĞRULANMIŞ FEM VE İSTATİSTİKSEL YAKLAŞIMLAR

Anahtar kelimeler

Çok katmanlı kaplamalı kesici takım, sonlu elemanlar yöntemi, gri ilişkisel analiz

Öz

Alüminyum bazlı Metal Matris Kompozitler (MMK), yüksek mukavemet, sertlik ve düşük ağırlık gibi daha iyi mekanik ve fiziksel özelliklerinden dolayı metal kesme uygulamalarında yaygın olarak kullanılmaktadır. Ayrıca, modern kaplama uygulamaları, özellikle çok katmanlı kaplamalı takımlar, kesici takım performanslarını iyileştirerek MMK'ları işleme konusundaki zorlukları ortadan kaldırmada üstün bir potansiyele sahiptir. Bu nedenle, çalışmada, doğrulanmış FEM ve istatistiksel yaklaşımla çok katmanlı kaplamalı semente karbür bir kesici takımın Al-4.5%Cu/TiB2/3p MMK'nın tornalama performansını ortaya çıkarmak amaçlanmıştır. Deneysel olarak kalibre edilmiş ve seçilmiş bir similasyon için farklı kalınlık ve dizilimlerde (iki adet yumuşak ve üç adet sert kaplama malzemesi için) istatiksel olarak similasyon tasarımı kurulmuştur. Gri İlişki Analizi (GRA) yardımı ile MMK malzemenin tornalanmasında çok katmanlı kaplamalı uç performansını kesme kuvvetlerinin bileşkesi (FR) ve maksimum uç sıcaklığı (Tmax) baz alınarak araştırılmıştır. Optimum çok katmanlı kaplama, kaplama malzemeleri faktörleri için 4-2-4-3-2 seviyelerinde bulunmuş olup bu koşul sırasıyla: tungsten disülfid (WS2), molibden disülfür (MoS2), titanyum nitrür (TiN), alüminyum oksit (Al2O3), ve titanyum karbo-nitrürdür (TiCN). Her bir faktörün katkı oranları, Genel Doğrusal Model (GLM) ile incelenmiş, WS2 ve Al2O3 kaplama malzemeleri için sırasıyla %47,13 ve %24,43 oranında anlamlı olduğu tespit edilmiştir. Gelecekte çok katmanlı kaplamalar, MMK'ların işlenmesindeki zorlukları aşmak için değerli bir çözüm olabilirler.

Araştırma Makalesi			Research Article		
Başvuru Tarihi	:	18.07.2023	Submission Date	:	18.07.2023
Kabul Tarihi	:	24.11.2023	Accepted Date	:	24.11.2023

1. Introduction

Metal Matrix Composite (MMC) materials are strengthened by adding a carbon-based or ceramic material into a metal matrix to provide superior properties such as corrosion resistance, mechanical strength, elasticity modulus, etc. (Gürbüz, Şenel, & Koç, 2015; Senel & Gürbüz, 2021). The preference for MMC materials for engineering applications is gradually increasing due to their superior properties such as high strength, high young modulus, high toughness, high impact strength, enhancement wear resistance, high hardness, and low weight (Radhika, Subramaniam, & Senapathi, 2013; Rathodi & Pandey, 2017). Aluminum MMCs are primarily used in the automotive and aerospace industries for better corrosion and wear resistance (Joel & Xavior, 2018). Aluminum-based MMCs are mainly enhanced with hard ceramics; thus, the MMCs become difficult-to-cut materials (J. P. Chen, Gu, & He, 2020; Nicholls, Boswell, Davies, & Islam, 2017; Radhika et al., 2013). Therefore, many recent studies have directed to machining Al MMCs enhanced with ceramics. The parameters, such as tool wear, workpiece surface roughness, cutting forces, insert tip temperature, chip formation, etc., can be investigated during the machining of MMCs. For example, silicon carbide (SiC) (Bhushan, 2021; Das & Chakraborty, 2018; Swain, Das Mohapatra, Das, Sahoo, & Panda, 2020), aluminum oxide (Al_2O_3) (Prakash & Iqbal, 2018), and boron carbide (B4C) (Channabasavaraja, Nagaraj, & Srinivasan, 2016; Hiremath, Auradi, & Dundur, 2016; Saravanan & Mahendran, 2020) reinforcement Al MMCs have been trend investigations recently.

Denkena, Tonshoff, & Boehnke (2005) investigated the machinability of iron-rich Al MMC regarding tool wear aspect due to their lower density and high oxidation resistance properties, which presented a high potential for automotive and aerospace applications. The claim that "Economic cutting operations are currently not possible" was revealed. Modern coating applications have become a cure to solve the economic problems of machining MMCs to investigate the insert performances regarding tool wear, cutting forces, cutting parameters and temperatures, etc. Uncoated carbide inserts caused built-up-edge and coating inserts like TiN, TiAIN, and CrN might not eliminate this weakness (P. Roy, Sarangi, Ghosh, & Chattopadhyay, 2009). Akgün, Özlü, & Kara (2023) investigated the effect of PVD-TiN and CVD-Al_2O_3 coatings on the hard turning of AISI H13. The authors revealed that the CVD-Al_2O_3 coated insert was more effective than the PVD-TiN coated insert regarding the abrasion and adhesion mechanisms. MoS2, a soft coating material, was used to solve the built-up edge and adhesion tendency by coating inserts (Harris, Vlasveld, Doyle, & Dolder, 2000). An investigation on tool wear performance during machining of SiC-reinforced ZA43 alloy MMC presented that coated tungsten carbide insert with triple layered with hard coating materials (Al_2O_3, TiN, and TiCN) performed better than uncoated one according to tool wear aspect (Marigoudar & Sadashivappa, 2014).

Multi-layered coating of the tools has innovative potential for cutting applications for heavy-duty conditions due to the friction and high heat energy during the machining. S. Roy & Ghosh (2014) investigated the high-speed turning of AISI 4140 steel using nano-tube-based nanofluid in minimum quantity lubrication (MQL) by a multi-layer (TiN-Al_2O_3-TiCN) coated insert. The nanofluid MQL machining performance was compared to wet and dry machining conditions and performed better than the others. During the machining of hardened steel at or above 50 HRC, multi-layer coated carbide inserts have outperformed compared to single-layered coated carbide inserts (Kene, Orra, & Choudhury, 2016). Kara, Aslantas, & Çiçek (2016) predicted the cutting temperature of coated (TiCN+Al2O3+TiN and Al_2O_3) uncoated inserts for orthogonal cutting of AISI 316 L by an artificial neural network. C. S. Kumar & Patel (2018a) focused on the machining performance comparison of mono-layered AlCrN and multi-layer AlTiN coated Al_2O_3/TiCN-based mixed ceramic insert in turning of hardened AISI 52100 steel (62 HRC hardness). Multi-layer AlTiN coated inserts performed better anti-oxidation, anti-adhesion, and anti-abrasive behaviors than mono-layered AlCrN coated and uncoated inserts. Also, C. S. Kumar & Patel (2018b) continued to search the coating thickness effect of mono-layered AlCrN, and multi-layer AlTiN coated Al_2O_3/TiCN-based mixed ceramic insert during the machining of hardened AISI 52100 steel. They revealed that multi-layer AlTiN coated inserts showed better adhesion to the substrate. Lian, Mu, Liu, Chen, & Yao (2019) presented an exciting soft/hard composite coating aspect for multi-layered coating literature. The main motto was "The external soft coating layer on the hard coating layer played a significant role in decreasing cutting forces and temperatures because the soft coating layer had lower shear strength than general insert materials." They also investigated the coating thickness and material effects on turning of AISI 1045 steel as a three-dimensional numerical simulation aspect. Then, they proposed that the Soft/hard composite coating thickness ratio should have been 0.9:0.1. R. Kumar et al. (2019) investigated the optimal cutting parameters for turning JIS S45C structural steel with the multi-layer coated (TiN-TiCN-Al_2O_3-TiN) carbide insert. They advised the optimal cutting parameters as cutting speed (Vc) 120 m/min, dept of cut (d) 0.3 mm, and feed (f)0.05 mm/rev regarding the tool flank wear, surface roughness of the workpiece, and chip morphology. Interestingly, Tooptong, Nguyen, Park, & Kwon (2021) revealed a unified crater wear model combining the abrasive wear and dissolution wear for the multi-layer (TiN-Al_2O_3-TiCN) coated carbide insert during the machining of flake graphite iron, compacted graphite iron, and nodular graphite iron. The maximum crater wear was measured experimentally, and 2D FEM simulations determined the maximum cutting temperatures to guess the contributions from abrasive and dissolution wear. The crater wear differences for the three types of iron came from

the cutting temperature differences. U. Kumar & Senthil (2020) investigated the machining performance of the multi-layer (TiN-AlTiN) coated tungsten carbide insert during the dry turning Ti-6Al-4V. The focused originality of the search was revealing the machining performance of the insert as deep cryogenic treated at -184 ºC for a period of 36 h and then tempering in an electrical furnace at 250 ºC for 6 hours. The cryogenic treatment achieved lesser surface roughness and cutting forces due to lowering the insert's thermal conductivity and increased wear resistance and hardness. In a recent study (Ranjan & Hiremath, 2022), 3D FEM simulation validated by the experiment of machining AISI 420 was performed using the multi-layer (TiN-TiCN-Al_2O_3-TiN, TiN- Al_2O_3- TiCN-TiN) coated and uncoated inserts. The coated inserts differed from each other regarding layer sequences and thickness of layers. The TiN-TiCN-Al_2O_3-TiN multi-layer coated carbide insert was found to be more effective than the other inserts regarding the minimum generation of effective stress, cutting temperature, and cutting power.

Numerous 2D FEM studies of MMCs can be found in the literature describing the tool-particle interaction, particle orientation, tool wear, etc., but a few 3D FEM studies have been investigated. Pramanik, Zhang, & Arsecularatne (2007) investigated tool-particle interaction based on geometrical orientation, tool wear, and surface damage during the machining of Al matric SiC particle reinforcement MMC using 2D FEM in the ANSYS/LS-DYNA software package. The particles were %20 by volume and were assumed to bond to the matrix perfectly. Stress/strain fields were determined for possible debonding and fracture. One of the limitations of the 2D FEM simulation was to challenge severe mesh distortion due to the nonuniform deformations in the chip removal. As a solution, chip formation was revealed by a self-designed continuous remeshing routine by modeling 2D orthogonal machining of Al/SiC MMC in the ABAQUS software package (Schulze, Zanger, Michna, Ambrosy, & Pabst, 2011). Another significant issue in the 2D FEM of the orthogonal machining MMCs was modeling the interface between reinforcement particles and base matrix. Umer et al. (2015) modeled the interface between reinforcement particles and base matrix using two concepts, with or without cohesive zone elements (CZE). The model could predict cutting forces, chip morphology, stresses, and temperatures by comparing CZE for Al/SiC MMC machining. CZE with a parting line approach was advised as the best model for the 2D FEM of the orthogonal machining to simulate serrated chips. Afterward, Ghandehariun, Kishawy, Umer, & Hussein (2016) modeled a 2D FEM of the orthogonal machining Al/Al_2O_3 MMC to reveal a more comprehensive knowledge of particle-matrix interaction. Three concepts for particles positioned along, above, and below the cutting line were successfully simulated with the CZE model. Umer, Kishawy, Ghandehariun, Xie, & Al-Ahmari (2017) continued their studies by focusing on tool performance (PCD) using 2D FEM of the orthogonal machining Al/Al_2O_3 and Al/SiC MMCs. While the model without CZE could accurately determine cutting

forces, tool stresses, and temperatures, the model with CZE could estimate the effect of matrix-particle interaction on tool stresses and machined surfaces. In addition, some recent studies did not choose the CZE for particle-matrix interactions for MMCs. Xiong, Wang, Jiang, Lin, & Shao (2018) focused on the 2D orthogonal cutting FEM of TiB2/7075Al MMC to investigate the chip formation mechanism. The matrix-particle interaction was defined by Python programming, and the uncut chip part was created as an isotropic monophasic part without particles to solve high mesh distortion and computing times. Despite the self-programming, the other common method was to use matrix element failure (the debonding energy defined as Johnson-Cook damage law) surrounding the reinforcement particles by assuming the particles were perfectly bonded to the matrix (Josyula & Narala, 2018; Umer, Abidi, Abu Qudeiri, Alkhalefah, & Kishawy, 2020). Although the summarized literature focused on the 2D FEM analysis, which lighted the mechanics and particle-matrix interactions of the cutting process, the 3D FEM studies related to the turning of MMCs have been limited. During hot turning, Jadhav & Dabade (2016) simulated 3D FEM of Al/SiCp (10 and 30 % SiC particles) MMCs. They used the Deform 3D software package. Vc, d, f, and preheating temperatures were chosen as effective parameters to investigate. They modeled the material regarding to Johnson-Cook material model and 3D equivalent homogeneous material model data. Another recent investigation (X. Chen, Xie, Xue, & Wang, 2017) cited that 2D FEM analysis has its own disadvantages, which end up inconsistency with experimental cutting forces, and relatively discontinuous chip morphology. Thus, a 3D equivalent homogeneous material model was developed for the SiCp/Al6063/30p MMC to simulate the milling process in the ABAQUS software package. The experimental verification was provided for milling forces and chip shape within the 20% error band.

3D FEM simulations can be significant for machining optimizations (Ugur, 2022), accurately estimating cutting forces (Baris & Levent, 2021) (especially for radial cutting force), investigating preheating and different coating technologies, etc. Furthermore, the abovementioned investigations have stood limited to evaluating the performance of multi-layer coated inserts in the machining of Al MMCs. Also, Al-4.5%Cu/TiB2/3p is a recently investigated MMC, especially its mechanical behavior due to its potential applications in the automobile and aerospace industries (Shaik Mozammil, Karloopia, Verma, & Jha, 2019; Shaik Mozammil, Koshta, & Jha, 2021; S. Mozammil, Koshta, Jha, & Swain, 2022). Based on the determined literature gap, the turning performance of a cemented carbide insert was investigated regarding the evaluation of multi-layer coated conditions under different coating thicknesses during the cutting Al-4.5%Cu/TiB2/3p MMC. Verified FEM and statistic approaches were used for the cutting performance, and optimum multi-layered coating types in terms of their sequence and thicknesses of each layer were revealed.

2. Materials and Methods

The insert's CAD design, FEM simulations for turning Al-4.5%Cu/TiB2/3p MMC, and the design of simulations for the multi-layered coating types in terms of their sequence and thicknesses were presented in detail in this section. Also, research and publication ethics were obeyed in this study.

2.1CAD Model for Insert

The cutting tool geometry was selected similarly to the literature, which used experimental results of the turning Al-4.5%Cu/TiB2/3p MMC to calibrate the FEM simulations. Although the insert type was not given in the study, a technical drawing of the insert and insert specifications (insert material, nose radius, rake angle, etc.) was proposed (S. Mozammil et al., 2022). Some unremarked dimensions needed to design a 3D CAD file were determined from the technical drawing of the insert via the ImageJ software package by calibrating with certain measurements. So, the insert's CAD design and geometrical dimensions were created in CATIA V5, as shown in Figure 1.

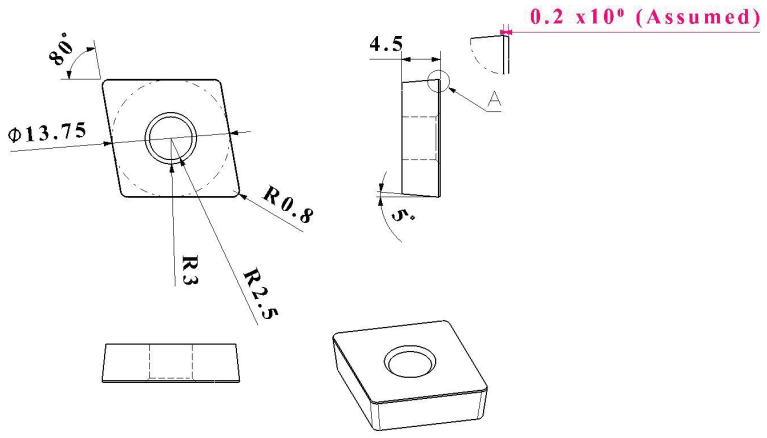

Figure 1. 2D Drawing and Isometric View of the Insert

2.2 FEM Simulations and Verification

A 3D FEM simulation was set by Deform 3D ver. 11.0 software package. A notebook with an eight-core 11th Gen Intel® Core™ I7 CPU, 32 GB RAM, and SSD technology performed all FEM simulations.

2.2.1 Geometric Characteristics of the Turning Process

The insert geometry was designed as shown in Figure 1. Also, the tool holder

specifications were selected regarding the experimental reference study (S. Mozammil et al., 2022). The inclination, rake, and tool cutting edge angles were set as -6,-6, and 95, respectively. The workpiece geometry for the chip removal path was selected as a circular arc with a diameter of 33 mm (S. Mozammil et al., 2022) and a 10^0 angle for the more realistic FEM simulation. Also, the workpiece was fixed by setting the zero velocity of the nodes in the Y-Z and X-Y axes for the bottom and back surfaces, respectively. Figure 2 summarizes the geometric characteristics of the turning process.

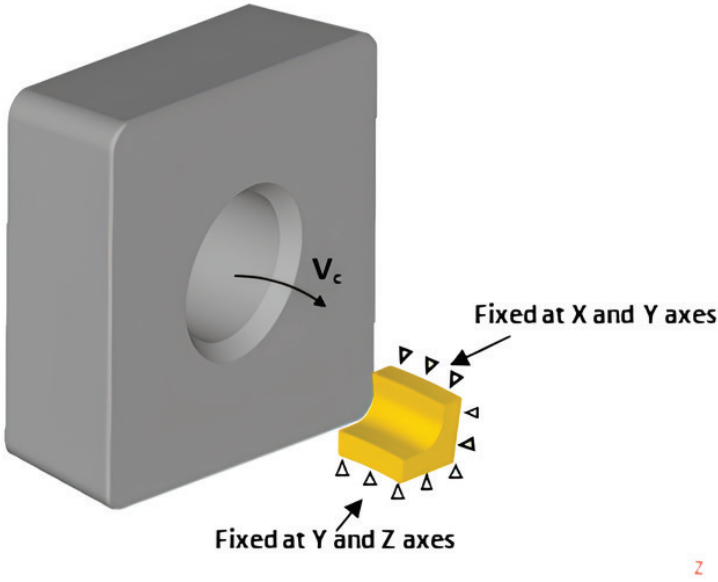

Figure 2. The Geometric Characteristic of the FEM Setup

2.2.2 Insert-Workpiece Interface

Meshing is counted as the most critical parameter for analyzing the 3D Flow of a complex cutting process, and adaptive meshing is required. DEFORM 3D can automatically optimize remeshing in the cutting region by controlling user-defined parameters such as the time step, mesh sizes, mesh elements, etc. Thus, the software was selected.

The 3D CAD model of the insert and simplified workpiece geometry regarding cutting parameters and nose radius are presented in Figure 1-2. The modeling of the insert was a rigid body with 25000 tetrahedral mesh elements. The size ratio of the meshes was 4:1 (Figure 3.a), and the insert tip meshed finer using a mesh window with a size ratio of 0.1 (Figure 3.b). A plastic body was appointed to the workpiece and meshed with 25% of the feed value. Also, the contact area of the

workpiece meshed as a 7:1 size ratio (Figure 3.c) to a finer result (Bathula, Buddi, Shagwira, Mwema, & Rajesh, 2022; Kyratsis, Tzotzis, Markopoulos, & Tapoglou, 2021; Ozturk, 2022; Tzotzis, Garcia-Hernandez, Huertas-Talon, & Kyratsis, 2020).

During the dry turning, the thermal boundary condition of the insert-workpiece interface was set as 0.02 $\frac{\text{N °C}}{\text{mm s}}$ for the convection coefficient, and 45 $\frac{\text{N °C}}{\text{mm s}}$ for the conduction heat transfer coefficient (Kyratsis et al., 2021; Ozturk, 2022; Tzotzis et al., 2020).

Finally, the friction condition at the insert-workpiece interface was set according to Coulomb's Law, which was the commonly used friction model for metalworking processes (Equation 1) (Bobrovskij, Khaimovich, Bobrovskij, Travieso-Rodriguez, & Grechnikov, 2022; Tan, 2002).

$$\tau_f = \mu\sigma n \tag{1}$$

Where τ_f indicates the frictional shear stress. μ shows the friction coefficient. Lastly, σ_n displays stress of the insert-workpiece interface. The reference study (S. Mozammil et al., 2022) proposed the friction coefficient for machining Al-4.5%Cu/TiB_2/3p MMC as 0.54. Therefore, μ was set to 0.54.

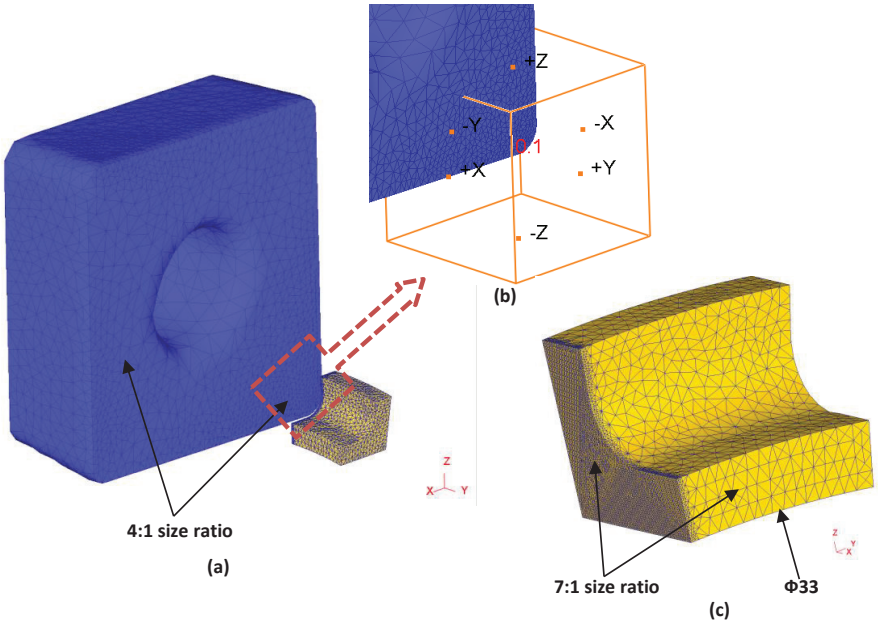

Figure 3. The Meshed Geometries (a) Insert, (b) Insert Tip, and (c) Workpiece

2.2.3 Material Models for Insert Workpiece and Coatings

2D FEM simulations have clarified significant knowledge about the mechanics of the cutting process, especially particle-matrix interactions. However, 3D FEM simulations can provide an evaluation of 3 components of the cutting forces more clearly, more helpful tool wear prediction, and more accurate information about stress, strain, displacement, and temperature behavior of the cutting interface, etc. Also, 3D FEM simulations for machining operations can be crucial for cutting tool marketing due to machining optimizations. Therefore, the recent literature has a trend to use 3D equivalent homogeneous material (EHM) models developed by constitutive material characteristics and failure criterion definitions for specific MMCs (X. Chen et al., 2017; Jadhav & Dabade, 2016).

The Johnson-Cook (JC) plasticity material model is the most common and well-known material model for the recent FEM studies of machining applications (İynen, Ekşi, Akyıldız, & Özdemir, 2021; Ch Sateesh Kumar, Zeman, & Polcar, 2020; Ozturk, 2022). JC model parameters were determined by constitutive material characteristics and material constants estimation for the Al-4.5%Cu/TiB2/3p MMC (S. Mozammil et al., 2022). JC model is described as follows:

$$\sigma = (A + B\varepsilon^n)\left(1 + C ln\frac{\dot{\varepsilon}}{\dot{\varepsilon_0}}\right)\left[1 - \left(\frac{T - T_0}{T_m - T_0}\right)^m\right] \quad (2)$$

The symbols $\sigma, \varepsilon, \dot{\varepsilon}, \dot{\varepsilon_0}, T, T_0, T_m$ represent a variety of quantities in the context of this study: equivalent stress, plastic strain, plastic strain rate, reference strain rate, reference temperature, ambient temperature, and melting temperature, respectively. Additionally, the symbols A, B, n, and m denote the empirical constants related to the workpiece material. These constants represent the initial yield stress, the strain hardening modulus, the strain hardening exponent, and the thermal softening exponent, respectively. The empirical parameters utilized in this study for the MMC were obtained from a previously published work (S. Mozammil et al., 2022). The parameters are also displayed in Table 1. Moreover, it was assumed that the reference strain rate for the simulations was 0.001/s.

Table 1. The JC material model values of Al-4.5%Cu/TiB2/3p MMC (S. Mozammil et al., 2022)

A (MPa)	**B (MPa)**	**C**	**n**	**m**	T_0	T_m **(Du, Eskin, & Katgerman, 2006)**
175	65.884	0.0165	0.1633	1.1711	27	570.8

Whereas the workpiece was set as a plastic body, the insert was selected as rigid.

Like the recent literature (Kyratsis et al., 2021; Ozturk, 2022), the normalized Cockcroft-Latham damage model was employed for the material fracture criterion. The thermo-mechanical features of the insert, coatings, and workpiece are presented in Table 2. The insert was chosen as the reference paper (S. Mozammil et al., 2022), and the thermo-mechanical properties were taken from the Deform 3D library concerning carbide (19% Cobalt)(Corporation, 2014). When appointing the mechanical properties of the Al-4.5%Cu/TiB2/3p MMC, the reference paper (S. Mozammil et al., 2022) was used. Nevertheless, the MMC's thermal properties have not yet been investigated in the literature. For this reason, the workpiece's thermal properties in the simulations were assumed from the Al-4.5%Cu as referencing previous studies (Choi, 2020; Du, Eskin, & Katgerman, 2006). In addition, coatings were employed for the insert with different thicknesses concerning the design of experiments. One of the coating applications is randomly exhibited in Figure 4.

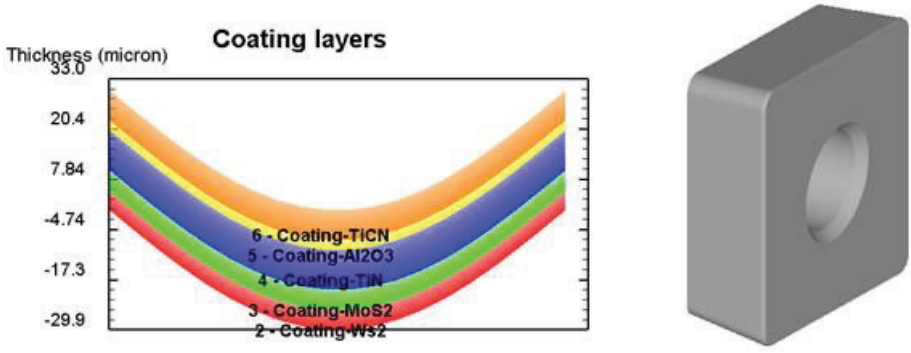

Figure 4. The Graphical View Of Coatings For the 13th of FEM Simulation

Table 2. Thermo-Mechanical Features of the İnsert (Corporation, 2014), Workpiece (Choi, 2020; Du et al., 2006; S. Mozammil et al., 2022), and Coatings (Lian et al., 2019; Ozturk, 2022; Ranjan & Hiremath, 2022; Vasiliev, 2021; Volovik et al., 1978)

Mechanical Properties	**Insert**	**MMC**	**WS_2**	**MoS_2**	**TiN**	**Al_2O_3**	**TiCN**
Young's modulus (GPa)	496.423	$72.14x10^{-3}$	354	330	600	415	448
Density (kg/m^3)	157	2764	7500	5060	4650	3780	4180
Poisson's ratio	0.24	0.31	0.28	0.125	0.25	0.22	0.23
Thermal Properties	**Insert**	**MMC (Assumed)**	**WS_2**	**MoS_2**	**TiN**	**Al_2O_3**	**TiCN**
Heat Capacity ($N/mm^{20}C$)	5.91	2.64	1.92	2.01	3	3.42	2.5
Thermal Expansion ($x\ 10^{-6}\ ^0C^{-1}$)	7.2	f(Temp.)	6.35	10.70	9.4	8.4	8
Thermal Conductivity (W/m^0C)	74.764	180	32	37	20 at 40 ^0C	33 at 50 ^0C	26 at 25 ^0C
					21 at 100 ^0C	28 at 90 ^0C	27 at 100 ^0C
					22 at 300 ^0C	19 at 300 ^0C	28 at 300 ^0C
					23.5 at 500 ^0C	13 at 500 ^0C	30.5 at 500 ^0C
					26 at 1000 ^0C	7 at 1000 ^0C	33.5 at 1000 ^0C
					27 at 1300 ^0C	7 at 1300 ^0C	35 at 1300 ^0C

2.3 Design of Simulations and Statistics Approach

Nine experiments, turning the Al-4.5%Cu/TiB2/3p MMC under different cutting conditions, were chosen from 27 experiments for the exact turning conditions (S. Mozammil et al., 2022). The nine experiments were selected because of their small broken chip formations like 10^0 angle FEM simulations for verification.

Then, four of them were chosen concerning the simple randomized method for the validation of FEM simulations. After that, the experiment with the lowest absolute error for the resultant cutting force was decided. It was explained in detail in Section 3.

This study was prepared to reveal the cemented carbide insert performance with multi-layered coating types in terms of their sequence and thicknesses of each layer. The factors were coating types, two of them soft coatings (WS2 and MoS2) and three of them hard coatings (TiN, Al2O3, and TiCN). All factors were evaluated with five levels. Then, twenty-five validated FEM simulations were performed as an L25 (55) orthogonal array. Table 3 shows the factors and levels. Table 4 presents the design of twenty-five validated FEM simulations. The selected cutting condition with the absolute minimum error was used for all simulations to compare multi-layered coating combinations. The selected cutting parameters were 995 rpm, 1.5 mm, and 0.14 $\frac{mm}{rev}$ or spindle speed (n), depth of cut (d), and feed (f), respectively (Table 5).

Table 3. Factors and Levels

Factors	Level 1	Level 2	Level 3	Level 4	Level 5
WS_2	UNCOATED	2.5 µm	5 µm	7.5 µm	10 µm
Mos_2	UNCOATED	2.5 µm	5 µm	7.5 µm	10 µm
TiN	UNCOATED	2.5 µm	5 µm	7.5 µm	10 µm
al_2o_3	UNCOATED	2.5 µm	5 µm	7.5 µm	10 µm
Ticn	UNCOATED	2.5 µm	5 µm	7.5 µm	10 µm

Table 4. L25 Orthogonal Array For Coating Types

Simulation No	WS_2	MOs_2	TiN	Al_2O_3	TiCN
1	1	1	1	1	1
2	1	2	2	2	2
3	1	3	3	3	3
4	1	4	4	4	4
5	1	5	5	5	5
6	2	1	2	3	4
7	2	2	3	4	5
8	2	3	4	5	1
9	2	4	5	1	2
10	2	5	1	2	3
11	3	1	3	5	2
12	3	2	4	1	3
13	3	3	5	2	4
14	3	4	1	3	5
15	3	5	2	4	1
16	4	1	4	2	5
17	4	2	5	3	1
18	4	3	1	4	2
19	4	4	2	5	3
20	4	5	3	1	4
21	5	1	5	4	3
22	5	2	1	5	4
23	5	3	2	1	5
24	5	4	3	2	1
25	5	5	4	3	2

Grey relation analysis (GRA) is a popular statistical model for determining the optimal parameters of a process considering multiple factors and variables.

The multiple responses calculated by obtaining data from Taguchi Orthogonal Array can be transformed into a single response in GRA to evaluate the similarity between different data (Kasemsiri, Dulsang, Pongsa, Hiziroglu, & Chindaprasirt, 2017; Sylajakumari, Ramakrishnasamy, & Palaniappan, 2018). Therefore, GRA

was used by following the steps below to investigate the effect of the multi-layered coatings types for the cemented carbide insert.

- **Grey Relation Generation:** It includes pre-processing data through the normalization of responses into two distinct groups: larger-the-better and smaller-the-better. Implementing the smaller-the-better criterion in this study is considered suitable to minimize the resultant cutting forces and tool temperatures.

  The normalized data can be calculated as shown in Equation 3 (Ozturk, 2022; Sylajakumari et al., 2018).

$$X_i = \frac{maxy_i(k) - y_i(k)}{maxy_i(k) - miny_i(k)} \tag{3}$$

  Where, X_i calculated value after Grey relation generation, $maxy_i\ (k)$ is the highest value of $y_i\ (k)$, $miny_i\ (k)$is the smallest value of the $y_i\ (k)$ and $y_i\ (k)$ is the ith response.

- **Determining of Grey Relation Coefficient (GRC)and Grade(GRG):** The subsequent procedure involves the computation of the GRC and the GRG using the following equations (Kasemsiri et al., 2017; Ozturk, 2022; Sylajakumari et al., 2018).

$$\Delta_{0i}(k) = |X_0(k) - X_i(k)| \tag{4}$$

  Where, $\Delta_{0i}\ (k)$, is the deviation, $X_0\ (k)$ is reference, and $X_i\ (k)$ is comparability. Then, the GRC can be calculated as Equation 5.

$$\mathcal{s}_i(k) = \frac{\Delta_{min} + \zeta\Delta_{max}}{\Delta_{0i}(k) + \zeta\Delta_{max}} \tag{5}$$

  Where, $s_i\ (k)$ and ζ represent the GRC of the individual response variables and the distinguish coefficient, defined within the interval ζ∈ [0,1]. It is generally assumed as 0.5. Then, the GRG is determined as below.

$$\varphi_i = \frac{1}{n}\sum_{i=1}^{n} \mathcal{s}_i(k) \tag{6}$$

In the above equation, φ_i represents the value of GRG, and n indicates the number of responses. Furthermore, the optimal level is determined and validated using the following equation.

$$\varphi_{predited} = \varphi_m + \sum_{i=1}^{q}(\varphi_0 - \varphi_m) \tag{7}$$

In the equation 7, φ_0 indicates the maximum GRG's average at the optimal level

of factor, φ_m displays the mean of GRG, and q is the number of factors influencing response values.

Finally, whether the contributions of the coating types with different thicknesses significantly affect the insert performance or not was determined by the General Linear Model (GLM) in Minitab Software.

3. Results

Figure 5 depicts a randomly selected cutting force graphic utilized in Finite Element Method (FEM) simulations of turning the Al-4.5%Cu/TiB2/3p. The simulations were carried out to estimate the three components of cutting force under various cutting conditions. When the force data obtained from the FEM simulations were transferred to a personal computer, the average value of the cutting forces was computed. Then, the resultant cutting forces (FR) were determined to compare with the experimental results (S. Mozammil et al., 2022). The experimental and predicted FR results are presented in Table 5. Also, the absolute errors of FR were calculated to appoint the simulation for the L25 orthogonal array. The selected FEM simulation, which has the absolute minimum error, is shown in yellow in Table 5.

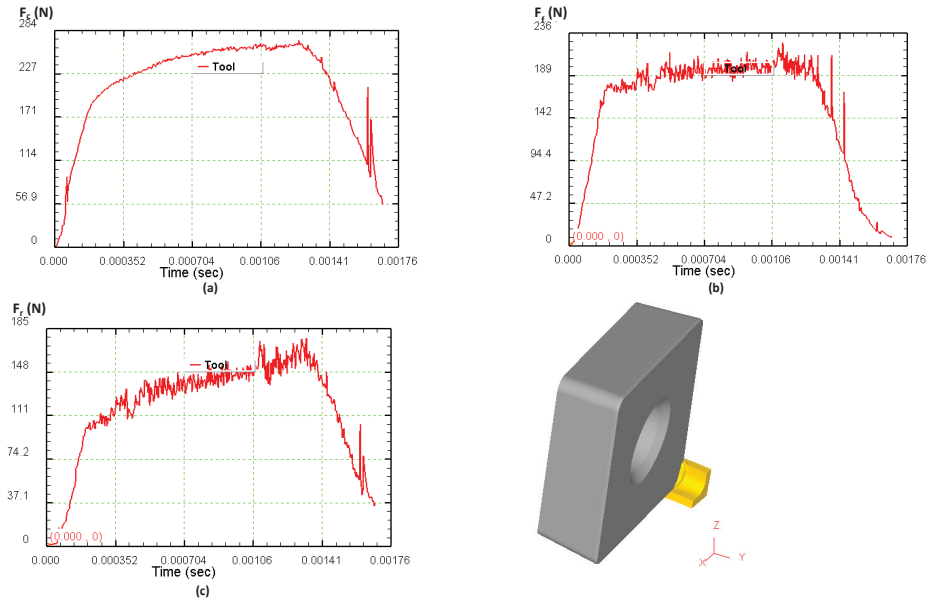

Figure 5. Cutting Force Components: (a) Main Cutting Force (Fc), (b) Feed Force (Ff), and Radial Force (Fr) (spindle speed, n=995 rpm, d=1.5 mm, and f=0.10 mm/rev)

Table 5. The comparison of Cutting Forces Between Experiments (S. Mozammil et al., 2022) and Predicted FEM Results

No	Cutting Parameters			Experiment Results				FEM Results				Absolute error (%)
	n (rpm)	d (mm)	f (mm/ rev)	F_c (N)	F_f (N)	F_r (N)	F_R (N)	F_c (N)	F_f (N)	F_r (N)	F_R (N)	
1	995	1.5	0.05	211.62	98.97	45.42	237.99	151.05	135.95	85.43	220.45	7.37
2	995	1	0.1	230.06	104.94	49.5	257.66	177.55	113.43	126.25	245.61	4.67
3	995	1.5	0.1	251.54	119.57	52.6	283.44	215.78	155.85	120.17	292.05	3.04
4	995	1.5	0.14	293.6	148.46	63.5	335.07	256.44	157.88	138.44	331.44	1.08

After the selection of the verified FEM simulation concerning the absolute minimum error (Table 5), the cutting performance of the multi-layer coated cemented carbide insert was evaluated regarding five different coating types in terms of their sequences and the five-level of thicknesses for each coating type. (Table 3). Then, the L25 (55) orthogonal array (Table 4) was built. Twenty-five simulations were set with the chosen cutting condition, then the FR and maximum insert temperature (Tmax) values were derived from FEM as output (Table 6). Next, The GRA statistical approach revealed the optimal multi-layered coating condition for turning Al-4.5%Cu/TiB2/3p MMC by evaluating the combined influences of the coatings on both FR and Tmax. The optimal condition for the GRA statistic model was found at levels 4-2-4-3-2 for WS2, MoS2, TiN, Al_2O_3, and TiCN, respectively, concerning the response table of mean GRGs (Table 7). As the mean of GRGs is higher, there is a stronger correlation (Ozturk, 2022; Sylajakumari et al., 2018). The optimal condition needed to be confirmed. Thus, the predicted optimal value of the multi-layered coating condition was calculated as Equation 7. Then, the simulation result for the optimal condition was compared with the expected optimal value, as shown in Table 8. They found good agreement with each other.

Although the GRA advised the optimum condition at levels 4-2-4-3-2 regarding FR and Tmax outputs, whether all the factors significantly affected the cutting performance or not had to be evaluated. Therefore, the influence of the factors on both FR and Tmax outputs was assessed by the General Linear Model (GLM) in the Minitab software package. The set ANOVA for GRGs is presented in Table 9. Since the probability values (p) of the WS2 and Al_2O_3 coatings were calculated as smaller than 0.05 reasonable alpha level, these coatings and their thicknesses were significantly the most influential factors for insert performance. Their contribution ratios are 47.13% and 24.43% for WS2 and Al_2O_3 coating, respectively. Also, the reasonable alpha levels of the other three factors were determined as higher than 0.05; thus, they had no significant influences on the cutting performance.

Table 6. The GRA Model for the Twenty-Five Verified Simulations Concerning F_R and T_{max} Outputs

								Normalization		Deviation Sequence		GRC			
Sim. No	**WS_2**	**MOs_2**	**TiN**	**Al_2O_3**	**TiCN**	**F_R (N)**	**T_{max} (^{0}C)**	**F_R (N)**	**T_{max} (^{0}C)**	**F_R (N)**	**T_{max} (^{0}C)**	**F_R (N)**	**T_{max} (^{0}C)**	**GRG**	**Rank**
1	1	1	1	1	1	331.44	112.55	0.3995	0.0000	0.6005	1.0000	0.4543	0.3333	0.3938	25
2	1	2	2	2	2	324.94	93.014	0.5284	0.6779	0.4716	0.3221	0.5146	0.6082	0.5614	21
3	1	3	3	3	3	333.02	89.56	0.3682	0.7977	0.6318	0.2023	0.4418	0.7120	0.5769	20
4	1	4	4	4	4	351.59	97.42	0.0000	0.5250	1.0000	0.4750	0.3333	0.5128	0.4231	24
5	1	5	5	5	5	319.05	98.2	0.6451	0.4979	0.3549	0.5021	0.5849	0.4990	0.5419	22
6	2	1	2	3	4	324.78	83.73	0.5315	1.0000	0.4685	0.0000	0.5163	1.0000	0.7581	4
7	2	2	3	4	5	338.08	85.95	0.2678	0.9230	0.7322	0.0770	0.4058	0.8665	0.6361	14
8	2	3	4	5	1	321.6	86.75	0.5946	0.8952	0.4054	0.1048	0.5522	0.8267	0.6895	5
9	2	4	5	1	2	329.41	86.76	0.4397	0.8949	0.5603	0.1051	0.4716	0.8263	0.6489	12
10	2	5	1	2	3	329.9	87.81	0.4300	0.8584	0.5700	0.1416	0.4673	0.7793	0.6233	15
11	3	1	3	5	2	339.61	86.89	0.2375	0.8904	0.7625	0.1096	0.3960	0.8201	0.6081	17

12	3	2	4	1	3	330.83	85.75	0.4116	0.9299	0.5884	0.0701	0.4594	0.8771	0.6682	8
13	3	3	5	2	4	317.81	91.7	0.6697	0.7235	0.3303	0.2765	0.6022	0.6439	0.6230	16
14	3	4	1	3	5	327.99	86.42	0.4679	0.9067	0.5321	0.0933	0.4844	0.8427	0.6636	10
15	3	5	2	4	1	322.52	87.15	0.5763	0.8813	0.4237	0.1187	0.5413	0.8082	0.6748	6
16	4	1	4	2	5	314.68	89.98	0.7318	0.7831	0.2682	0.2169	0.6508	0.6975	0.6742	7
17	4	2	5	3	1	301.15	86.52	1.0000	0.9032	0.0000	0.0968	1.0000	0.8378	0.9189	1
18	4	3	1	4	2	314.87	84.68	0.7280	0.9670	0.2720	0.0330	0.6477	0.9382	0.7929	3
19	4	4	2	5	3	327.06	90.35	0.4863	0.7703	0.5137	0.2297	0.4933	0.6852	0.5892	18
20	4	5	3	1	4	318.3	88.9	0.6600	0.8206	0.3400	0.1794	0.5952	0.7360	0.6656	9
21	5	1	5	4	3	336.74	92.84	0.2944	0.6839	0.7056	0.3161	0.4147	0.6127	0.5137	23
22	5	2	1	5	4	316.75	90.35	0.6907	0.7703	0.3093	0.2297	0.6178	0.6852	0.6515	11
23	5	3	2	1	5	321.79	88.81	0.5908	0.8237	0.4092	0.1763	0.5499	0.7394	0.6446	13
24	5	4	3	2	1	323.13	92.54	0.5642	0.6943	0.4358	0.3057	0.5343	0.6206	0.5775	19
25	5	5	4	3	2	312.18	84.88	0.7813	0.9601	0.2187	0.0399	0.6957	0.9261	0.8109	2

Table 7. Response Table For Means

Level	WS_2	MOs_2	TiN	Al_2O_3	TiCN
1	0,4994	0,5896	0,6250	0,6042	0,6509
2	0,6712	0,6872	0,6456	0,6119	0,6844
3	0,6475	0,6654	0,6128	0,7457	0,5943
4	0,7282	0,5804	0,6532	0,6081	0,6243
5	0,6396	0,6633	0,6493	0,6160	0,6321
Delta	0,2287	0,1068	0,0403	0,1414	0,0902
Rank	1	3	5	2	4

Table 8. Confirmation of GRA

	Predicted result for optimal condition	Simulation result for optimal condition
GRG value	0.8366	0.8100

Table 9. The Contribuitons of the GRGs Via ANOVA

Factors	DF	Seq SS	Contribution	Adj SS	Adj MS	F-Value	P-Value
WS_2	4	0,142638	47,13%	0,142638	0,035659	13,69	0,013
MoS_2	4	0,047333	15,64%	0,047333	0,011833	4,54	0,086
TiN	4	0,006072	2,01%	0,006072	0,001518	0,58	0,693
Al_2O_3	4	0,073937	24,43%	0,073937	0,018484	7,10	0,042
TiCN	4	0,022278	7,36%	0,022278	0,005570	2,14	0,240
Error	4	0,010420	3,44%	0,010420	0,002605		
Total	24	0,302678	100,00%				

4. Discussion

The usage of Al-based MMCs for engineering applications in automotive and aerospace industries is gradually increasing due to their superior mechanical and physical properties (Joel & Xavior, 2018; Radhika et al., 2013; Rathodi & Pandey, 2017). Thus, their machining behaviors are still investigated to perform economic and efficient cutting processes (Denkena et al., 2005; Harris et al., 2000; Marigoudar & Sadashivappa, 2014; P. Roy et al., 2009). Multi-layered coating of the tools has innovative potential concerning various cutting applications in previous studies, especially the machining of difficult-to-machine metals. For example, the literature revealed that the multi-layered coated inserts performed better than uncoated and single-layer coated inserts for hardened steels such as AISI 4140 (S. Roy & Ghosh, 2014), AISI 52100 (C. S. Kumar & Patel, 2018a) as showing superior

anti-oxidation, anti-adhesion, and anti-abrasive behaviors. In addition, the FEM simulation of the MMCs can be useful in determining the machining behaviors of the MMCs. The studies have trended to 2D FEM studies to reveal the tool-particle interaction, particle orientation, tool wear, etc. (Ghandehariun et al., 2016; Josyula & Narala, 2018; Pramanik et al., 2007; Schulze et al., 2011; Umer et al., 2020; Umer et al., 2015; Umer et al., 2017; Xiong et al., 2018). However, the 3D FEM studies related to the turning of MMCs have been limited (X. Chen et al., 2017; Jadhav & Dabade, 2016) and can be significant for machining optimizations, accurately estimating cutting forces, cutting conditions, and different coating technologies. For that reason, the 3D FEM and statistic-based study investigated the turning performance of different multi-layer coated cemented carbide inserts under different coating thicknesses during the cutting Al-4.5%Cu/TiB2/3p MMC.

The strengths of this study can be collected as (1) verified 3D FEM simulation, (2) revealing the performance of the insert coated by multi-layer with different soft and hard ones, and lastly, (3) all simulations were built concerning the design of experiments and evaluated by specific statistical methods. The 3D Fem simulations were calibrated by the data from the previous experimental study (S. Mozammil et al., 2022). The best agreement cutting condition between experiments and simulations was chosen. However, the MMC's thermal properties have not yet been investigated in the literature, and the thermal properties of the MMC were assumed from the Al-4.5%Cu referencing previous studies (Choi, 2020; Du et al., 2006). This assumption can be thought of as a limitation of this study. The thermal performance of the insert was just used for comparing the various multi-layered coatings' effects during the same cutting conditions, so this assumption has not provided a problem in evaluating the coatings' effects. The CAD geometry of the insert was modeled without the chip breaker, whereas the original insert geometry was. This insert model can be a limitation, but the randomly selected experiments agreed well with the FEM simulation concerning the FR values. Also, this limitation was minimized by choosing the absolute minimum error between experiments and simulations, so it won't be a real limitation to evaluate the multi-layered coatings' effects on the insert performance.

Soft/hard coatings can perform better since the soft top layer provides an interface film in the friction process, and the hard bottom layer increases wear resistance (Lian et al., 2019). This study revealed a similar result to this motto. Whereas the WS2 is the soft coating material with a low friction coefficient, the Al_2O_3 has a higher hardness, improving the wear resistance. The most influential factors affecting the insert performance were found in WS2 and Al_2O_3 coatings, with contribution ratios are 47.13% and 24.43%, respectively.

5. Conclusion

This study investigated the machining performance of cemented carbide inserts,

which were multi-layer coated by different materials concerning various thicknesses during the turning of Al-4.5%Cu/TiB2/3p MMC. The aim was to prove the performance effect of the multi-layer coated with soft and hard materials on the cemented carbide inserts using a verified FEM approach and statistics.

After the 3D FEM simulation was approved and the design of simulations was set, the GRA was built to reveal the optimum multi-layered coating condition regarding both FR and Tmax output results. In addition, the contribution rates of each coating material were investigated by GLM. The design of simulations has two types of levels; one is no coating, and the four have coating materials with various thickness levels. Thus, this model determined the optimal condition by comparing multi-layered coatings and no-coating situations. The optimal condition for the GRA statistic model was found at levels 4-2-4-3-2 for WS2, MoS2, TiN, Al_2O_3, and TiCN, respectively. Moreover, WS2 and Al_2O_3 coatings were found to be the most influential factors affecting the insert performance, with 47.13% and 24.43% contribution ratios, respectively. The multi-layered coatings can be an effective solution for machining the MMCs.

Not many studies have been investigated concerning the abovementioned literature. The verified 3D Fem and statistic-based study has been a new perspective for machining aluminum MMCs by multi-layer coated inserts. This study was limited to certain factors such as specific workpiece and coating materials, particular insert type, and fixed machining conditions; however, changes in these factors, how/whether influence the cutting performance of a MMC or not, can be investigated in further studies.

Acknowledgment

Any foundation did not financially support this study. All the steps of this study were set and performed by the author.

Conflict of Interest

The author reports that there are no competing interests to declare.

References

Akgün, M., Özlü, B., & Kara, F. (2023). Effect of PVD-TiN and CVD-Al_2O_3 Coatings on Cutting Force, Surface Roughness, Cutting Power, and Temperature in Hard Turning of AISI H13 Steel. *Journal of Materials Engineering and Performance, 32*(3), 1390-1401. doi: https://link.springer.com/article/10.1007/s11665-022-07190-9

Baris, O., & Levent, U. (2021). Optimization of cutting forces on turning of Ti-6Al-4V Alloy by 3D FEM simulation analysis. *Journal of Engineering Research and Applied Science, 10*(2). Retrieved from https://www.journaleras.com/index.php/jeras/article/view/256

Bathula, D. B., Buddi, T., Shagwira, H., Mwema, F. M., & Rajesh, K. V. D. (2022). Analysis on behavior of Ti-6al-4v & Ti-5553 by performing turning operation using deform-3d. *Advances in Materials and Processing Technologies,* 1-18. doi: https://doi.org/10.1080/2374068X.2022.2037064

Bhushan, R. K. (2021). Multi-Response Optimization of Parameters during Turning of AA7075/SiC Composite for Minimum Surface Roughness and Maximum Tool Life. *Silicon,* 13(9), 2845-2856. doi: https://link.springer.com/article/10.1007/s12633-020-00640-w

Bobrovskij, I., Khaimovich, A., Bobrovskij, N., Travieso-Rodriguez, J. A., & Grechnikov, F. (2022). Derivation of the Coefficients in the Coulomb Constant Shear Friction Law from Experimental Data on the Extrusion of a Material into V-Shaped Channels with Different Convergence Angles: New Method and Algorithm. *Metals,* 12(2). doi: https://doi.org/10.3390/met12020239

Channabasavaraja, H. K., Nagaraj, P. M., & Srinivasan, D. (2016). Determination of Optimum Cutting Parameters for Surface Roughness in Turning AL-B4C Composites. *International Conference on Advances in Materials and Manufacturing Applications (Iconamma-2016), 149.* doi: https://iopscience.iop.org/article/10.1088/1757-899X/149/1/012029

Chen, J. P., Gu, L., & He, G. J. (2020). A review on conventional and nonconventional machining of SiC particle-reinforced aluminium matrix composites. *Advances in Manufacturing, 8*(3), 279-315. doi: https://link.springer.com/article/10.1007/s40436-020-00313-2

Chen, X., Xie, L., Xue, X., & Wang, X. (2017). Research on 3D milling simulation of SiCp/Al composite based on a phenomenological model. *The International Journal of Advanced Manufacturing Technology, 92*(5), 2715-2723. doi: https://doi.org/10.1007/s00170-017-0315-0

Choi, S. W. (2020). Influences of Precipitation of Secondary Phase by Heat Treatment on Thermal Properties of Al-4.5%Cu Alloy. *KOREAN JOURNAL OF MATERIALS RESEARCH,*30(8), 435-440. doi: https://doi.org/10.3740/MRSK.2020.30.8.435

Corporation, S. F. T. (2014). Deform, Version 11.0 (PC);.

Das, D., & Chakraborty, V. (2018). Dry condition machining performance of T6 treated aluminium matrix composites. *Materials Today-Proceedings, 5*(9), 20145-20151. doi: https://doi.org/10.1016/j.matpr.2018.06.383

Denkena, B., Tonshoff, H. K., & Boehnke, D. (2005). An assessment of the machinability of iron-rich iron-aluminium alloys. *Steel Research International, 76*(2-3), 261-264. doi: https://doi.org/10.1002/srin.200506007

Du, Q., Eskin, D., & Katgerman, L. (2006). Modelling macrosegregation during DC

casting of a binary aluminium alloy. *Modeling of Casting, Welding and Advanced Solidification Processes - XI, 1,* 235-242. doi: https://link.springer.com/article/10.1007/s11661-006-9042-0

Ghandehariun, A., Kishawy, H. A., Umer, U., & Hussein, H. M. (2016). Analysis of tool-particle interactions during cutting process of metal matrix composites. *International Journal of Advanced Manufacturing Technology, 82*(1-4), 143-152. doi: https://link.springer.com/article/10.1007/s00170-015-7346-1

Gürbüz, M., Şenel, M. C., & Koç, E. (2015). Grafen takviyeli alüminyum matrisli yeni nesil kompozitler. [New generation composites with graphene reinforced aluminum matrix]. *Mühendis ve Makina, 56*(669), 36-47. Retrieved from https://dergipark.org.tr/en/pub/muhendismakina/issue/54339/736188

Harris, S. G., Vlasveld, A. C., Doyle, E. D., & Dolder, P. J. (2000). Dry machining - commercial viability through filtered arc vapour deposited coatings. *Surface & Coatings Technology, 133,* 383-388. doi: https://doi.org/10.1016/S0257-8972(00)00895-1

Hiremath, V., Auradi, V., & Dundur, S. T. (2016). Experimental Investigations on Effect of Ceramic B4C Particulate Addition on Cutting Forces and Surface Roughness during Turning of 6061Al Alloy. *Transactions of the Indian Ceramic Society, 75*(2), 126-132. doi: https://doi.org/10.1080/0371750X.2016.1164626

İynen, O., Ekşi, A. K., Akyıldız, H. K., & Özdemir, M. (2021). Real 3D turning simulation of materials with cylindrical shapes using ABAQUS/Explicit. *Journal of the Brazilian Society of Mechanical Sciences and Engineering, 43*(8), 374. doi: https://doi.org/10.1007/s40430-021-03075-5

Jadhav, M. R., & Dabade, U. A. (2016). *Modelling and Simulation of Al/SiCp MMCs During Hot Machining.* Paper presented at the ASME 2016 International Mechanical Engineering Congress and Exposition. doi: https://doi.org/10.1115/IMECE2016-66071

Joel, J., & Xavior, M. A. (2018). Aluminium Alloy Composites and its Machinability studies; *A Review. Materials Today-Proceedings, 5*(5), 13556-13562. doi: https://doi.org/10.1016/j.matpr.2018.02.351

Josyula, S. K., & Narala, S. K. R. (2018). Study of TiC particle distribution in Al-MMCs using finite element modeling. *International Journal of Mechanical Sciences, 141,* 341-358. doi: https://doi.org/10.1016/j.ijmecsci.2018.04.004

Kara, F., Aslantas, K., & Çiçek, A. (2016). Prediction of cutting temperature in orthogonal machining of AISI 316L using artificial neural network. A*pplied Soft Computing, 38,* 64-74. doi: https://doi.org/10.1016/j.asoc.2015.09.034

Kasemsiri, P., Dulsang, N., Pongsa, U., Hiziroglu, S., & Chindaprasirt, P. (2017).

Optimization of Biodegradable Foam Composites from Cassava Starch, Oil Palm Fiber, Chitosan and Palm Oil Using Taguchi Method and Grey Relational Analysis. *Journal of Polymers and the Environment, 25*(2), 378-390. doi: https://link.springer.com/article/10.1007/s10924-016-0818-z

Kene, A. P., Orra, K., & Choudhury, S. K. (2016). Experimental Investigation of Tool Wear Behavior of Multi-Layered Coated Carbide Inserts Using Various Sensors in Hard Turning Process. *Ifac Papersonline, 49*(12), 180-184. doi: https://doi.org/10.1016/j.ifacol.2016.07.592

Kumar, C. S., & Patel, S. K. (2018a). Effect of chip sliding velocity and temperature on the wear behaviour of PVD AlCrN and AlTiN coated mixed alumina cutting tools during turning of hardened steel. *Surface & Coatings Technology, 334,* 509-525. doi: https://doi.org/10.1016/j.surfcoat.2017.12.013

Kumar, C. S., & Patel, S. K. (2018b). Investigations on the effect of thickness and structure of AlCr and AlTi based nitride coatings during hard machining process. *Journal of Manufacturing Processes, 31,* 336-347. doi: https://doi.org/10.1016/j.jmapro.2017.11.031

Kumar, C. S., Zeman, P., & Polcar, T. (2020). A 2D finite element approach for predicting the machining performance of nanolayered TiAlCrN coating on WC-Co cutting tool during dry turning of AISI 1045 steel. *Ceramics International, 46*(16, Part A), 25073-25088. doi: https://doi.org/10.1016/j.ceramint.2020.06.294

Kumar, R., Modi, A., Panda, A., Sahoo, A. K., Deep, A., Behra, P. K., & Tiwari, R. (2019). Hard Turning on JIS S45C Structural Steel: An Experimental, Modelling and Optimisation Approach. *International Journal of Automotive and Mechanical Engineering, 16*(4), 7315-7340. doi: https://doi.org/10.15282/ijame.16.4.2019.10.0544

Kumar, U., & Senthil, P. (2020). Performance of cryogenic treated multi-layer coated WC insert in terms of machinability on titanium alloys Ti-6Al-4V in dry turning. *Materials Today-Proceedings, 27,* 2329-2333. doi: https://doi.org/10.1016/j.matpr.2019.09.122

Kyratsis, P., Tzotzis, A., Markopoulos, A., & Tapoglou, N. (2021). CAD-Based 3D-FE Modelling of AISI-D3 Turning with Ceramic Tooling. *Machines, 9*(1). doi: https://doi.org/10.3390/machines9010004

Lian, Y. S., Mu, C. L., Liu, M., Chen, H. F., & Yao, B. (2019). Three-dimensional numerical simulation of soft/hard composite-coated textured tools in dry turning of AISI 1045 steel. *Advances in Manufacturing, 7*(2), 133-141. doi: https://link.springer.com/article/10.1007/s40436-019-00249-2

Marigoudar, R. N., & Sadashivappa, K. (2014). Comparison of tool life and surface characteristics of uncoated, coated carbide and ceramic tools during mac-

hining of SiC reinforced ZA43 alloy MMC. *Materials Science and Technology, 30*(8), 876-887. doi: https://doi.org/10.1179/1743284713Y.0000000484

Mozammil, S., Karloopia, J., Verma, R., & Jha, P. K. (2019). Effect of varying TiB2 reinforcement and its ageing behaviour on tensile and hardness properties of in-situ Al-4.5%Cu-xTiB2 composite. *Journal of Alloys and Compounds, 793,* 454-466. doi: https://doi.org/10.1016/j.jallcom.2019.04.137

Mozammil, S., Koshta, E., & Jha, P. K. (2021). Abrasive Wear Investigation and Parametric Process Optimization of in situ Al–4.5%Cu–xTiB2 Composites. *Transactions of the Indian Institute of Metals, 74*(3), 629-648. doi: https://doi.org/10.1007/s12666-020-02180-8

Mozammil, S., Koshta, E., Jha, P. K., & Swain, P. K. (2022). Investigation on Experimental Machinability & 3D Finite Element Turning Simulations of Al-4.5%Cu/TiB2/3p Composite. *Transactions of the Indian Institute of Metals.* doi: https://doi.org/10.1007/s12666-022-02735-x

Nicholls, C. J., Boswell, B., Davies, I. J., & Islam, M. N. (2017). Review of machining metal matrix composites. *International Journal of Advanced Manufacturing Technology, 90*(9-12), 2429-2441. doi: https://link.springer.com/article/10.1007/s00170-016-9558-4

Ozturk, E. (2022). FEM and statistical-based assessment of AISI-4140 dry hard turning using micro-textured insert. *Journal of Manufacturing Processes, 81,* 290-300. doi: https://doi.org/10.1016/j.jmapro.2022.06.060

Prakash, M., & Iqbal, U. M. (2018). Parametric optimization in turning of AA2014/Al_2O_3 nano composite for machinability assessment using sensors. *2nd International Conference on Advances in Mechanical Engineering (Icame 2018), 402.* doi: https://iopscience.iop.org/article/10.1088/1757-899X/402/1/012013

Pramanik, A., Zhang, L. C., & Arsecularatne, J. A. (2007). An FEM investigation into the behavior of metal matrix composites: Tool-particle interaction during orthogonal cutting. *International Journal of Machine Tools & Manufacture, 47*(10), 1497-1506. doi: https://doi.org/10.1016/j.ijmachtools.2006.12.004

Radhika, N., Subramaniam, R., & Senapathi, S. B. (2013). Machining parameter optimisation of an aluminium hybrid metal matrix composite by statistical modelling. *Industrial Lubrication and Tribology, 65*(6), 425-435. doi: https://www.emerald.com/insight/content/doi/10.1108/ILT-01-2011-0008/full/html

Ranjan, P., & Hiremath, S. S. (2022). Finite element simulation and experimental validation of machining martensitic stainless steel using multi-layered coa-

ted carbide tools for industry-relevant outcomes. S*imulation Modelling Practice and Theory, 114.* doi: https://doi.org/10.1016/j.simpat.2021.102411

Rathodi, B. S., & Pandey, B. (2017). Effect of Turning Parameters on Aluminium Metal Matrix Composites -A Review. International Conference on Materials, *Alloys and Experimental Mechanics (Icmaem-2017), 225.* doi: https://iopscience.iop.org/article/10.1088/1757-899X/225/1/012276

Roy, P., Sarangi, S. K., Ghosh, A., & Chattopadhyay, A. K. (2009). Machinability study of pure aluminium and Al-12% Si alloys against uncoated and coated carbide inserts. *International Journal of Refractory Metals & Hard Materials, 27*(3), 535-544. doi: https://doi.org/10.1016/j.ijrmhm.2008.04.008

Roy, S., & Ghosh, A. (2014). High-speed turning of AISI 4140 steel by multi-layered TiN top-coated insert with minimum quantity lubrication technology and assessment of near tool-tip temperature using infrared thermography. *Proceedings of the Institution of Mechanical Engineers Part B-Journal of Engineering Manufacture, 228*(9), 1058-1067. doi: https://doi.org/10.1177/0954405413514570

Saravanan, K. K., & Mahendran, S. (2020). Aluminium 6082-boron carbide composite materials preparation and investigate mechanical-electrical properties with CNC turning. *Materials Today-Proceedings, 21,* 93-97. doi: https://doi.org/10.1016/j.matpr.2019.05.368

Schulze, V., Zanger, F., Michna, J., Ambrosy, F., & Pabst, R. (2011). Investigation of the machining behavior of metal matrix composites (MMC) using chip formation simulation. *Modelling of Machining Operations, 223,* 20-29. doi: https://doi.org/10.4028/www.scientific.net/AMR.223.20

Senel, M. C., & Gürbüz, M. (2021). Investigation on Mechanical Properties and Microstructure of B4C/Graphene Binary Particles Reinforced Aluminum Hybrid Composites. *Metals and Materials International, 27*(7), 2438-2449. doi: https://link.springer.com/article/10.1007/s12540-019-00592-w

Swain, P. K., Das Mohapatra, K., Das, R., Sahoo, A. K., & Panda, A. (2020). Experimental investigation into characterization and machining of Al plus SiCp nano-composites using coated carbide tool. *Mechanics & Industry, 21*(3). doi: https://doi.org/10.1051/meca/2020015

Sylajakumari, P. A., Ramakrishnasamy, R., & Palaniappan, G. (2018). Taguchi Grey Relational Analysis for Multi-Response Optimization of Wear in Co-Continuous Composite. *Materials, 11*(9). doi: https://doi.org/10.3390/ma11091743

Tan, X. C. (2002). Comparisons of friction models in bulk metal forming. *Tribo-*

logy International, 35(6), 385-393. doi: https://doi.org/10.1016/S0301-679X(02)00020-8

Tooptong, S., Nguyen, D., Park, K. H., & Kwon, P. (2021). Crater wear on multi-layered coated carbide inserts when turning three distinct cast irons. *Wear, 484.* doi: https://doi.org/10.1016/j.wear.2021.203982

Tzotzis, A., Garcia-Hernandez, C., Huertas-Talon, J. L., & Kyratsis, P. (2020). Influence of the Nose Radius on the Machining Forces Induced during AISI-4140 Hard Turning: A CAD-Based and 3D FEM Approach. *Micromachines, 11*(9). doi: https://doi.org/10.3390/mi11090798

Ugur, L. (2022). A Numerical and Statistical Approach of Drilling Performance on Machining of Ti-6Al-4V Alloy. *Surface Review and Letters, 29*(12). doi: https://doi.org/10.1142/S0218625X22501682

Umer, U., Abidi, M. H., Abu Qudeiri, J., Alkhalefah, H., & Kishawy, H. (2020). Tool Performance Optimization While Machining Aluminium-Based Metal Matrix Composite. *Metals, 10*(6). doi: https://doi.org/10.3390/met10060835

Umer, U., Ashfaq, M., Qudeiri, J. A., Hussein, H. M. A., Danish, S. N., & Al-Ahmari, A. R. (2015). Modeling machining of particle-reinforced aluminum-based metal matrix composites using cohesive zone elements. *International Journal of Advanced Manufacturing Technology, 78*(5-8), 1171-1179. doi: https://link.springer.com/article/10.1007/s00170-014-6715-5

Umer, U., Kishawy, H., Ghandehariun, A., Xie, L. J., & Al-Ahmari, A. (2017). On modeling tool performance while machining aluminum-based metal matrix composites. *International Journal of Advanced Manufacturing Technology, 92*(9-12), 3519-3530. doi: https://link.springer.com/article/10.1007/s00170-017-0368-0

Vasiliev, O. O. (2021). Thermodynamic Properties of Tungsten Disulfide from First Principles in Quasi-Harmonic Approximation. *Powder Metallurgy and Metal Ceramics, 59*(9-10), 576-584. doi: https://link.springer.com/article/10.1007/s11106-021-00185-6

Volovik, L. S., Fesenko, V. V., Bolgar, A. S., Drozdova, S. V., Klochkov, L. A., & Primachenko, V. F. (1978). Enthalpy and heat capacity of molybdenum disulfide. *Soviet Powder Metallurgy and Metal Ceramics, 17*(9), 697-702. doi: https://doi.org/10.1007/BF00796559

Xiong, Y. F., Wang, W. H., Jiang, R. S., Lin, K. Y., & Shao, M. W. (2018). Mechanisms and FEM Simulation of Chip Formation in Orthogonal Cutting In-Situ TiB2/7050Al MMC. *Materials, 11*(4). doi: https://doi.org/10.3390/ma11040606